



Large Hadron Collider Project

LHC Project Report 1148

LHC TRANSVERSE FEEDBACK SYSTEM AND ITS HARDWARE COMMISSIONING

P. Baudrenghien, E. V. Gorbachev¹⁾, W. Hofle, F. Killing, I. Kojevnikov, G. Kotzian,
N. I. Lebedev¹⁾, R. Louwse, A. A. Makarov¹⁾, E. Montesinos, S. V. Rabtsun¹⁾, V. Rossi,
M. Schokker, E. Thepenier, D. Valuch, V. Zhabitsky¹⁾
CERN, Geneva, Switzerland

Abstract

A powerful transverse feedback system (“Damper”) has been installed in LHC. It will stabilise coupled bunch instabilities in a frequency range from 3 kHz to 20 MHz and at the same time damp injection oscillations originating from steering errors and injection kicker ripple. The transverse damper can also be used as an exciter for purposes of abort gap cleaning or tune measurement. The power and lowlevel systems layouts are described along with results from the hardware commissioning. The achieved performance is compared with earlier predictions and requirements for injection damping and instability control.

¹⁾ JINR, Dubna, Russia

Presented at
EPAC'08, 11th European Particle Accelerator Conference, Genoa, Italy - June 23-27, 2008

CERN,
CH-1211 Geneva 23
Switzerland



LHC TRANSVERSE FEEDBACK SYSTEM AND ITS HARDWARE COMMISSIONING

P. Baudrenghien, W. Höfle*, F. Killing, I. Kojevnikov, G. Kotzian, R. Louwerse, E. Montesinos, V. Rossi, M. Schokker, E. Thepenier, D. Valuch, CERN, Geneva, Switzerland
E.V. Gorbachev, N.I. Lebedev, A. A. Makarov, S.V. Rabtsun, V.M. Zhabitsky, JINR, Dubna, Russia

Abstract

A powerful transverse feedback system (“Damper”) has been installed in LHC. It will stabilise coupled bunch instabilities in a frequency range from 3 kHz to 20 MHz and at the same time damp injection oscillations originating from steering errors and injection kicker ripple. The transverse damper can also be used as an exciter for purposes of abort gap cleaning or tune measurement. The power and low-level systems layouts are described along with results from the hardware commissioning. The achieved performance is compared with earlier predictions and requirements for injection damping and instability control.

INTRODUCTION

The powerful transverse feedback system (“Damper”) for the Large Hadron Collider (LHC) is a joint project of the European Organization for Nuclear Research (CERN) and the Joint Institute for Nuclear Research (JINR) [1]. To a large extent this project is based on the system in the SPS [2] which has operated successfully for many years, facing in recent years, the additional challenge from the electron cloud effect [3].

The LHC will provide high intensity proton and lead ion beams. The ultimate intensities after injection into the LHC will be about $4.8 \cdot 10^{14}$ particles for the proton beam with an energy of 450 GeV and $4.1 \cdot 10^{10}$ ions for the $^{208}\text{Pb}^{82+}$ beam with an energy of 177 GeV/u. These intensities can lead to coherent transverse instabilities. The theoretical prediction for the instability rise time τ_{inst} , dominated at injection energy by the resistive wall effect, is about 18.5 ms or 208 turns [4] with a significant contribution of the LHC collimators at collision energy [5]. The LHC Damper will stabilize the beam against coupled bunch instabilities as well as damp the transverse oscillations of the beam originating from steering errors and kicker ripple. It will also be used for the purposes of tune measurement similar to the SPS system [6] and for abort gap cleaning [7].

GENERAL DESCRIPTION

The LHC Damper has 4 feedback systems on 2 circulating beams (one feedback system per beam and plane). Each system is a classical bunch-by-bunch transverse feedback system (TFS, see Fig. 1) [8]. It consists of 2 pick-ups (PU), 4 damper kickers (DK) and an electronic feedback

path with appropriate signal transmission from PU to DK. The DK corrects the transverse momentum of a bunch in proportion to its displacement from the closed orbit at the PU location. The digital signal processing unit (DSPU) ensures a resonance condition and an optimal phase advance ψ_{PK} to achieve the optimum damping. The mixing of signals from 2 pick-ups allows adjustment of the betatron oscillation phase advance from the “virtual” PU to the DK to an odd multiple of $\pi/2$. The total delay τ_{delay} in the signal processing of the feedback path from PU to DK adjusts the timing of the signal to match the bunch arrival time. It equals τ_{PK} , the particle flight of time from PU to DK, plus an additional delay of q turns:

$$\tau_{\text{delay}} = \tau_{\text{PK}} + qT_{\text{rev}}, \quad (1)$$

where T_{rev} is the revolution period of a particle in the synchrotron. The PU and DK are installed at locations with high β -functions. For vertical oscillations in the LHC (see Fig. 1), the delay τ_{delay} is slightly *smaller* than one beam revolution period $T_{\text{rev}} = 88.93 \mu\text{s}$ and $q_v = 0$. For the horizontal systems, kicker *downstream* of the PU, an additional delay of one turn ($q_H = 1$) is added. The delay τ_{delay} is then slightly *larger* than one turn.

The damping time $\tau_d = 40 T_{\text{rev}}$ of the LHC feedback was chosen to limit the emittance growth due to injection errors [9, 10]:

$$\frac{\Delta\epsilon}{\epsilon} = \frac{e_{\text{inj}}^2}{2\sigma^2} F_\epsilon; \quad F_\epsilon = \left(1 + \frac{\tau_{\text{dec}}}{\tau_d} - \frac{\tau_{\text{dec}}}{\tau_{\text{inst}}}\right)^{-2}, \quad (2)$$

where $e_{\text{inj}} \lesssim 4 \text{ mm}$ at $\beta = 185 \text{ m}$ (3.5σ) is the maximum assumed amplitude of a beam deviation from the closed orbit due to displacement and angular errors at injection; σ is the initial RMS beam size; $\tau_{\text{dec}} \simeq 750 T_{\text{rev}} = 68 \text{ ms}$ is the assumed decoherence time. These parameters lead to $\Delta\epsilon/\epsilon < 2.5\%$ the maximum admissible emittance blow-up in the LHC allocated to injection dipole errors [4]. Thus, the LHC TFS gain is $g = 2T_{\text{rev}}/\tau_d = 0.05$ and the overall damping time $1/\tau_d - 1/\tau_{\text{inst}}$ of the injection oscillations becomes about 50 turns or 4.4 ms.

The gain g and the maximum injection error e_{inj} yield the maximum deflection $\theta_{\text{max}} = 2 \mu\text{rad}$ required for the proton beam with energy 450 GeV and the location of the kickers at $\beta_k \gtrsim 100 \text{ m}$. The deflection θ_{max} is delivered by a set of electrostatic kickers with an aperture of 52 mm. The total required deflecting length of 6 m is divided into 4 kickers to limit the capacitive loading of the power amplifiers. The nominal voltage up to 1 MHz is $V_{\text{max}} \pm 7.5 \text{ kV}$.

* Wolfgang.Hofle@cern.ch

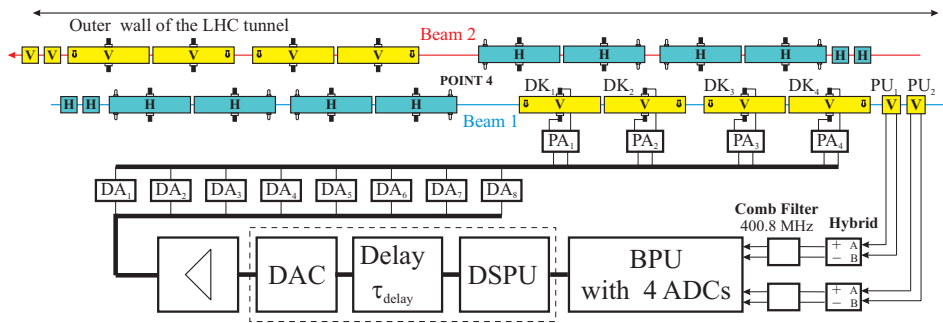


Figure 1: Layout of the LHC Damper and block diagram of the transverse feedback system for vertical oscillations.

The main instability that the feedback has to handle is the resistive wall instability for which the lowest frequency in the LHC is about 8 kHz ($Q_H = 64.28$ and $Q_V = 59.31$). For purposes of abort gap cleaning the unwanted beam should be coherently excited at frequencies of about 3 kHz and 8 kHz which correspond to the non-integer parts of the tune. Consequently a lower cut-off frequency of 1 kHz was chosen for the feedback loop. The highest frequency must be sufficient to damp the dipole mode of two neighbouring bunches. For the nominal bunch spacing of 25 ns $f_{max} = 20$ MHz. Coherent oscillations at higher frequencies are assumed to be suppressed by Landau damping. The pulse response must cope with the minimum gap between batches in the LHC (995 ns).

FEEDBACK ELECTRONICS

The Low Level part consists of two VME modules. For each PU a hybrid generates the difference and sum signals (see Fig. 1). Strip-line comb filters generate 400.8 MHz wavelets which are then processed by the Beam Position module. Its RF front-end consists of I/Q demodulators with the LO at the RF frequency, that produce (I,Q) pairs. After sampling at the bunch synchronous frequency of 40.08 MHz (16 bit ADCs) the signals, an FPGA calculates the transverse position of each bunch. These signals are then passed, via a 1 Gbps serial link, to the second VME module, the Digital Signal Processing Unit [11]. This latter module receives the transverse position data streams measured in two pick-ups. After deserialization the data are processed by an FPGA clocked at 80.16 MHz, with the following functionalities: Closed orbit rejection (notch filter), pick-up vector sum, one-turn delay (with 20 ps resolution), phase equalisation of the non-linear response of the amplifier and control of the loop bandwidth, low pass cut-off at 20 MHz. Finally a 14 bit DAC provides the output signal. Both modules include on board memory to acquire critical signals for observation and post-mortem.

ELECTROSTATIC KICKERS

The electrostatic kicker [1] consists of: a) a vacuum tank of stainless steel 304L, 1.6 m length, $\varnothing 100$ mm internal diameter and 14 mm wall thickness for optimal shielding

of electromagnetic fields at low frequency and for mechanical stability; b) an electrode module with two electrodes (shaped from copper strips as 90° arcs) and 3 ceramic-metal rings (metallization by a thin layer of rhenium to evacuate any charges) to hold the electrodes and align of the electrode module inside the vacuum tank; c) two high voltage feedthroughs; d) two couplers capacitively coupled to the electrodes to damp high order modes which can be excited by the beam and lead to instability. The estimated



Figure 2: Kickers and amplifiers in the LHC tunnel.

power loss to each electrode from the circulating ultimate beam current is 2 W/m. Tests under vacuum have shown that the temperature reaches 70°C when the electrodes are heated with 10 W/m [1]. This allows considerable margin for extra heat loss due to electron cloud. Tests of the kickers confirmed their compliance with design specifications. Tolerances on the 100 mm tank internal diameter are in the range of $0 \dots +0.054$ mm, camming actions of main flanges ($\varnothing 152$ mm) do not exceed 0.016 mm, the internal surface smoothness obtained is $R_a = 0.4 \mu\text{m}$. Standard vacuum cleaning procedures were used with a bake-out limited to $< 200^\circ\text{C}$ due to the copper electrodes. The pressure limits ($S = 30 \text{ l/s}$ for hydrogen) range from $2 \cdot 10^{-10}$ Torr to $1.7 \cdot 10^{-9}$ Torr for the eight installed kicker modules. These results are better than expectations based on an outgasing rate of $4 \cdot 10^{-12}$ mbar $\cdot \text{l/s}$ and a surface area estimated at $2 \cdot 10^4 \text{ cm}^2$, with an expected limit pressure of $2.6 \cdot 10^{-9}$ Torr.

POWER AND DRIVER AMPLIFIERS

16 power amplifiers (PA) are installed directly under 16 electrostatic kickers (DK) in the LHC tunnel on either side of Point 4 (see Fig. 1 and Fig. 2). Each pair of electrodes is driven in counter phase by one wideband power amplifier, consisting of two 30 kW grounded cathode tetrodes operated in class AB (push-pull). At low frequency the amplifier works on a relatively large impedance ($\sim 1 \text{ k}\Omega$) leading to a large kick voltage. At higher frequency the capacitance of the kicker plates shunts the impedance and consequently less kick strength is available. Every power amplifier is driven by two solid state driver amplifiers (DA) operating in class A. The maximum gain of the power amplifiers has been measured to be between 39 dB with a RS-2048-CJC tetrode (Thales®). The power amplifier is equipped with an RF voltage divider sensing the tetrode anode RF voltage. The higher order mode couplers (HOM) can also be used to measure accurately the voltage at the kicker plates. The HOM couplers consist of a 50Ω vacuum feedthrough with a small plate attached that capacitively couples to the kicker deflecting plates. The coupling capacitance of 6.4 pF and the 50Ω loading at the HOM form a high pass with a cut-off of $f_{\text{HP}} = 50 \text{ MHz}$. The first two higher order modes are at 89 MHz and at 176 MHz with an $R/Q \simeq 2 \dots 3 \Omega$ and a damped Q of 256 and 110, respectively. The transfer function from kicker voltage to the voltage measured at the HOM port when loaded with 50Ω is $F = jf/f_{\text{HP}}/(1 + jf/f_{\text{HP}})$. Fig. 3 shows

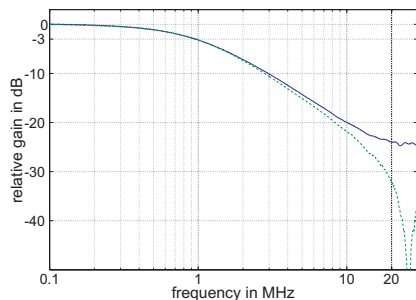


Figure 3: Power amplifier frequency characteristics: roll-off of gain for kicker voltage (solid) and tetrode anode voltage (dashed).

the relative gain versus frequency measured at the anode of the tetrode (dashed) and at the HOM port, corrected for the high pass response (solid). The latter represents the voltage seen by the beam as a function of frequency. At the anode of the tetrode the gain characteristic exhibits a resonance at $\sim 25 \text{ MHz}$ caused by the inductance of the connection to the kicker and the kicker capacitance. This resonance (notch in gain curve) is not seen on the kicker voltage transfer function. The measured phase response using the HOM ports and correcting for the high pass characteristics is shown in Fig. 4 together with the phase response as measured at the anode of the tetrode. Below 3 MHz the phase responses measured via the HOM ports and on

the anode voltage dividers perfectly match. The mismatch above 3 MHz is again caused by the resonance. The phase response will be compensated by an FIR in the digital signal processing part by adding phase at higher frequency in order to achieve an overall linear phase and constant group delay [11].

Power amplifiers and kickers are now all installed in the LHC tunnel and the system is undergoing extensive testing in the run-up for beam commissioning. The design specifications have all been met, the available peak voltage, 10.5 kV at up to 100 kHz, has exceeded the design value of 7.5 kV, giving a comfortable operational margin.

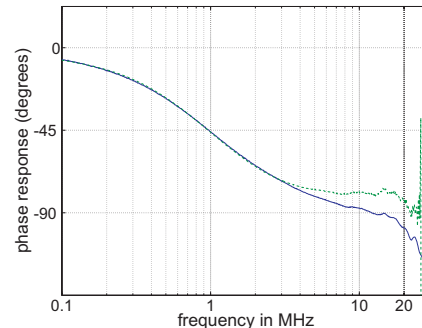


Figure 4: Phase response of power amplifier kicker ensemble, kicker voltage (solid), tetrode anode voltage (dashed).

ACKNOWLEDGMENTS

The authors thank T. Linnecar (CERN) for the helpful assistance and support for the project and the many colleagues of CERN and LPP (JINR) groups, in particular for vacuum, survey and installation.

REFERENCES

- [1] E. Gorbachev et al. PAC'01, June 2001, Chicago, Ill. (USA), pp. 1237–1239 (2001).
- [2] R. Bossart, L. Burnod, J. Gareyte, B. de Raad, V. Rossi, IEEE, Transactions on Nuclear Science, NIM, vol. NS-26, No. 3, pp. 3284–3286 (1979).
- [3] W. Höfle, Chamonix XI, January 2001, CERN-SL-2001-003-DI, CERN, Geneva, pp. 117–124 (2001).
- [4] O. S. Brüning et al. (Ed.) The LHC Design Report vol. I, CERN-2004-003, CERN, Geneva (2004).
- [5] E. Métral et al., PAC'07, June 2007, Albuquerque, NM (USA), pp. 2003–2005 (2007).
- [6] R. Bossart, V. Rossi, SPS-Improvement-Report-No-156, CERN-SPS-ABM-RB-jf, CERN, Geneva (1979).
- [7] A. Koschik et al., WEPP060, EPAC'08, Genova, June 2008, WEPP060, These Proceedings (2008).
- [8] L. Vos. IEEE, Transactions on Nuclear Science, NIM A, vol. 391, p. 56 (1996).
- [9] L. Vos. EPAC '98, June 1998, Stockholm, pp. 1365–1367 (1998).
- [10] V.M. Zhabitsky. Physics of Particles and Nuclei Letters, JINR, Dubna, 2008, vol. 5, No. 1(143), pp. 49–53 (2008).
- [11] P. Baudrenghien, G. Kotzian, W. Höfle, V. Rossi, THPC122, EPAC'08, Genova, June 2008, These Proceedings (2008).